Interpretation and Fracture Characterization of Upper Cretaceous Buda Limestone Formation Using Post-Stack 3D Seismic Data in Zavala County, Texas*

Andrey Smirnov[1] and Christopher L. Liner[1]

Search and Discovery Article #11108 (2018)**
Posted September 17, 2018

*Adapted from oral presentation given at 2018 AAPG Annual Convention & Exhibition, Salt Lake City, Utah, May 20-23, 2018
 DOI:10.1306/11108Smirnov2018

[1]Geosciences, University of Arkansas, Fayetteville, Arkansas (andrey.smirnov95@gmail.com)

Abstract

The Buda Limestone is a naturally fractured Upper Cretaceous carbonate formation in south Texas which unconformably underlies the Eagle Ford Shale. Matrix porosity of the Buda is less than 6%, therefore natural fractures improve the potential for commercial hydrocarbon production from this tight limestone formation. This presents a challenge for producers to identify these zones using well log and post-stack 3D seismic data typically available to medium or small exploration companies. This project provides a workflow based on well log analysis tied to seismic acoustic impedance (AI) inversion to locate areas of probable natural fractures.

Acoustic impedance inversion was performed across a 40 square mile 3D seismic survey. The AI data shows low AI shadow zones on the down-thrown side of faults. Post-stack geometric seismic attributes such as coherence, maximum and minimum curvature were analyzed in the anomalous AI areas, along with physical seismic attributes such as instantaneous amplitude and instantaneous frequency. This study indicates that a combination of acoustic impedance inversion and seismic attributes can identify areas of enhanced natural fracturing within the Buda Limestone interval.

Selected References

Ak, O., 2015, The depositional environment and the diagenetic processes of the Buda limestone (Cenomanian) in south-central Texas: Doctoral dissertation, The University of Texas at San Antonio.

Asquith, G., and D. Krygowski, 2004, Basic Well Log Analysis: AAPG Methods in Exploration Series, No. 16.

Bahorich, Mike, and Steve Farmer, 1995, 3-D seismic discontinuity for faults and stratigraphic features: The coherence cube: The Leading Edge, v. 14/10, p. 1053-1058.

Barnes, A.E., 2016, Appendix B: Hilbert Transform: Handbook of Poststack Seismic Attributes, p. 207-210.

Bennett, L.C., 2015, Interpretation of Late Cretaceous Volcanic Mounds and Surrounding Gulfian Series Formations Using 3D Seismic Data in Zavala County, Texas: M.S. Thesis, University of Arkansas.

Chopra S., and J. Marfurt, 2007, Volumetric curvature attributes adding value to 3D seismic data interpretation: SEG Technical Program Expanded Abstracts.

Chopra S., and J. Marfurt, 2010, Seismic attributes for prospect identification and reservoir characterization: Society of Exploration Geophysicists.

Chopra, S., and J. Marfurt, 2011, Interesting directions being pursued in seismic curvature attribute analysis: Canadian Society of Exploration Geophysicist, v. 36/4.

Far, M.E., C.M. Sayers, L. Thomsen, D.H. Han, and J.P. Castanga, 2013, Seismic characterization of naturally fractured reservoirs using amplitude versus offset and azimuth analysis: Geophysical Prospecting, v. 61/2, p. 427-447.

Ferrill, D.A., and A.P. Morris, 2008, Fault zone deformation controlled by carbonate mechanical stratigraphy, Balcones fault system, Texas: AAPG Bulletin, v. 92/3, p. 359-380.

Hardage, B., 2010, Instantaneous Seismic Attributes Calculated by the Hilbert Transform: Search and Discovery Article #40563 (2010). http://www.searchanddiscovery.com/documents/2010/40563hardage/index.htm?q=%2BtextStrip%3A40563

Holman, R. 2014, Seismic Characterization of Fractured Rock Fabric in Mississippian Limestone, Payne County, Oklahoma: M.S. Thesis, Oklahoma State University.

Lindseth, R.O., 1979, Synthetic sonic logs - a process for stratigraphic interpretation: Geophysics, v. 44/1, p. 3-26.

Najmuddin, Ilyas Juzer, 2003, Austin chalk fracture mapping using frequency data derived from seismic data: Doctoral Dissertation, Texas A&M University.

Ogiesoba, O., and U. Hammes, 2014, Seismic-attribute identification of brittle and TOC-rich zones within the Eagle Ford Shale, Dimmit County, South Texas: Journal of Petroleum Exploration and Production Technology, v. 4/2, p. 133-151. Doi: 10.1007/s13202-014-0106-1

Ouenes, A., T.C. Anderson, D. Klepacki, A. Bachir, D. Boukhelf, G.C. Robinson, and V.W. Stamp, 2010, Integrated characterization and simulation of the fractured Tensleep reservoir at Teapot Dome for CO_2 injection design: Society of Petroleum Engineers.

Quijada, M.F., 2009, Estimating elastic properties of sandstone reservoirs using well logs and seismic inversion: M.S Thesis, University of Calgary.

Roberts, A., 2001, Curvature attributes and their application to 3D interpreted horizons: First Break, v. 19/2, p. 85-100. doi:10.1046/j.0263-5046.2001.00142.x

Rose, P.R., 2016, Late Cretaceous and Tertiary burial history, Central Texas: Gulf Coast Association of Geological Societies, v.5, p. 141-179.

Russell, B., and D. Hampson, 1991, A comparison of post-stack seismic inversion methods: 61st Annual International Meeting, SEG, Expanded Abstracts, p. 876-878.

Sarhan, M.A., 2017, The efficiency of seismic attributes to differentiate between massive and non-Massive carbonate successions for hydrocarbon exploration activity: NRIAG Journal of Astronomy and Geophysics, v. 6/2, p. 311-325.

Simm, R., and M. Bacon, 2014, Seismic amplitude: an interpreter’s handbook: Cambridge University Press.

Yenugu, M., and K.J Marfurt, 2011, Relation between seismic curvatures and fractures identified from image logs - application to the Mississippian reservoirs of Oklahoma, USA: SEG Technical Program Expanded Abstracts 2011. doi:10.1190/1.3628240

Interpretation and Fracture Characterization of Upper Cretaceous Buda Limestone Formation Using Post-Stack 3D Seismic Data in Zavala County, Texas

Data Provided by Stephens Production Company

By Andrey Smirnov and Dr. Christopher Liner

ACE 2018 Annual Convention & Exhibition
ACE 101: Bridging Fundamentals and Innovation

Key Takeaways

- The Buda play is based on location of naturally fractured zones
- This research proposes that naturally fractured zones can be identified by utilizing post stack attributes in combination with acoustic impedance inversion
- Based on this research, naturally fractured zones tend to be associated with down-thrown sides of a fault

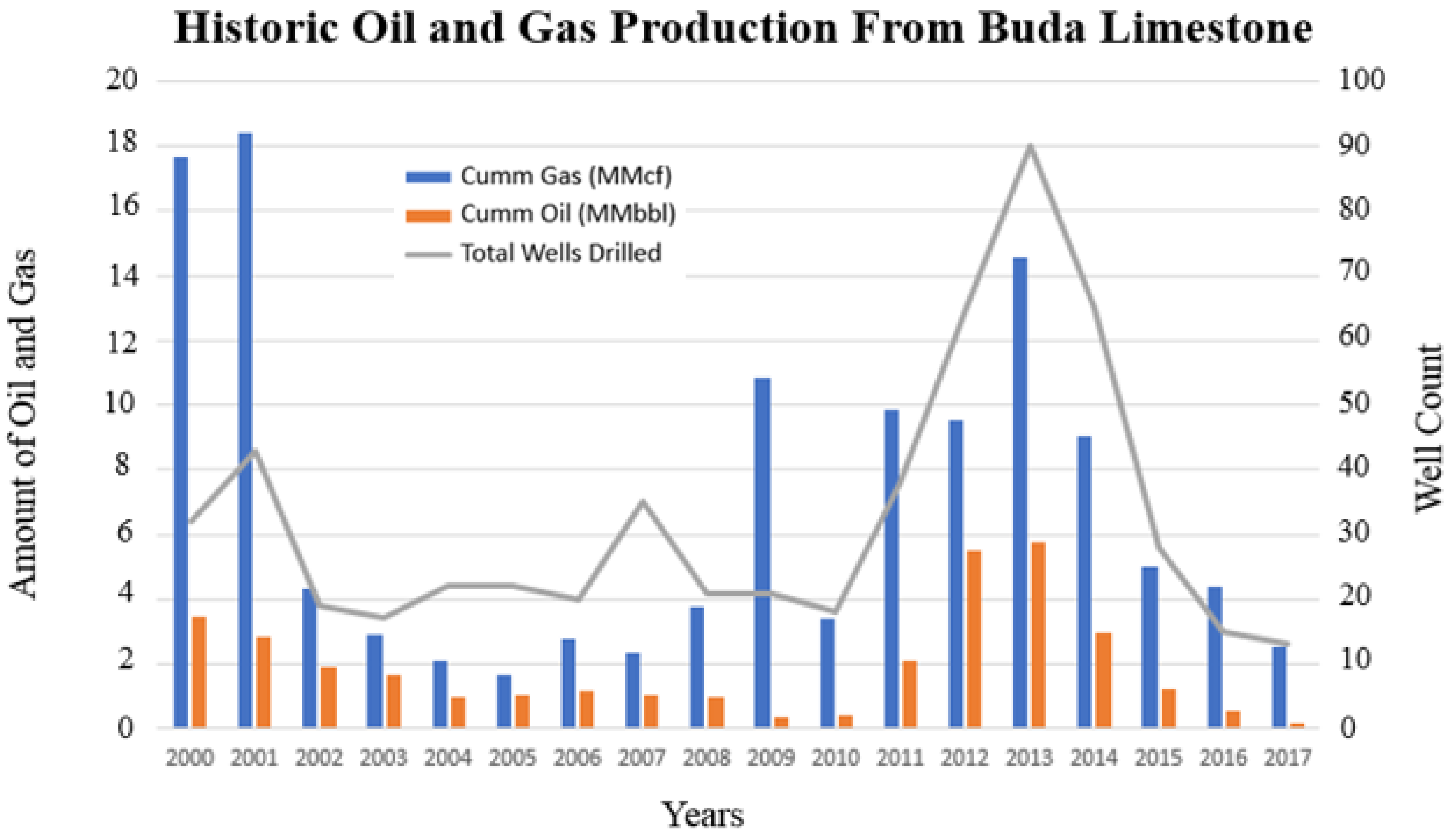

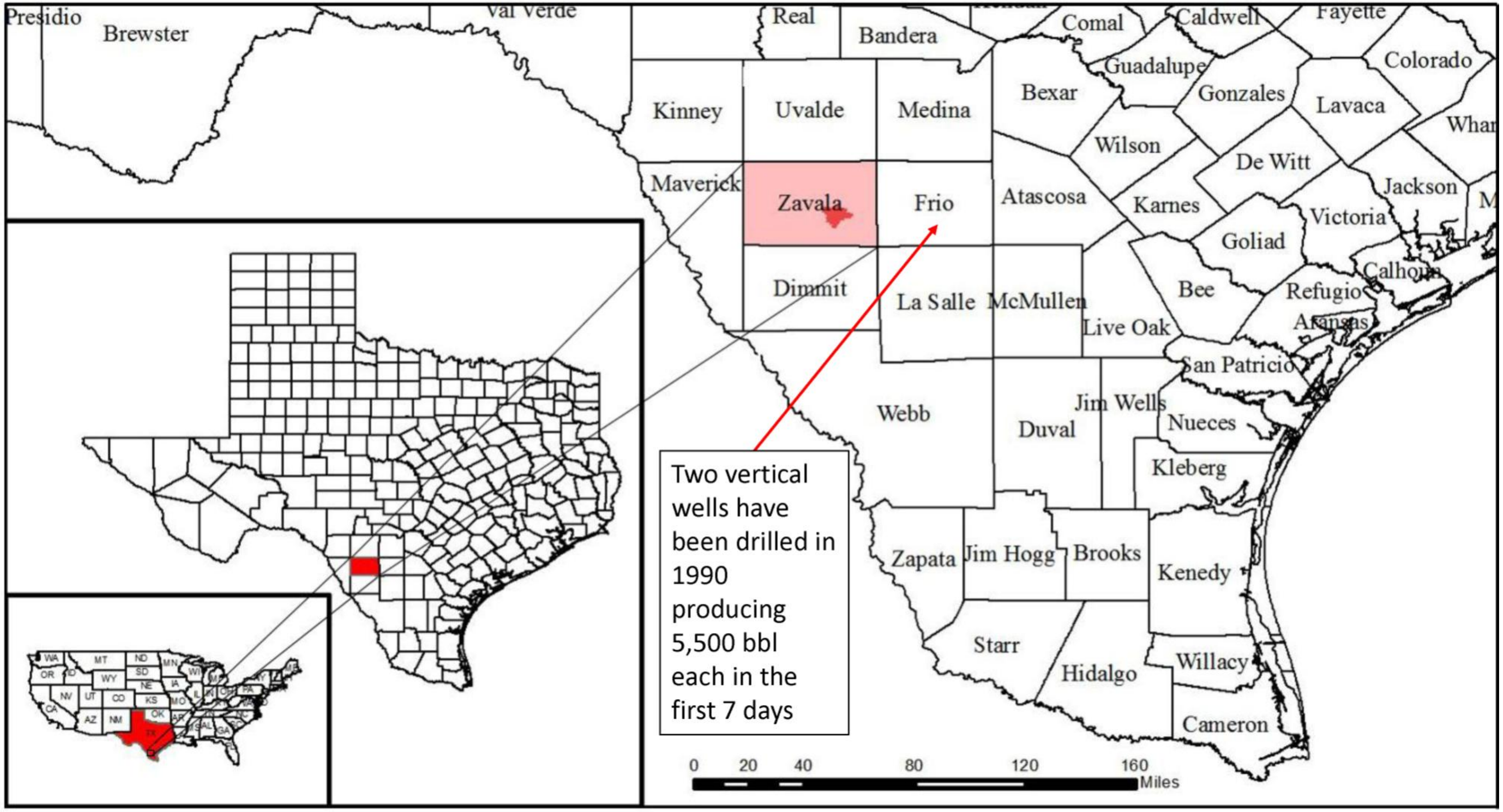

Presenter's notes: 3D Study area in Zavala County, Texas with 3D seismic survey outline (68 sq. mi.).

Presenter's notes: Late Albian stage of Early Cretaceous period just before the Buda Limestone was deposited (Wheat, 2014)

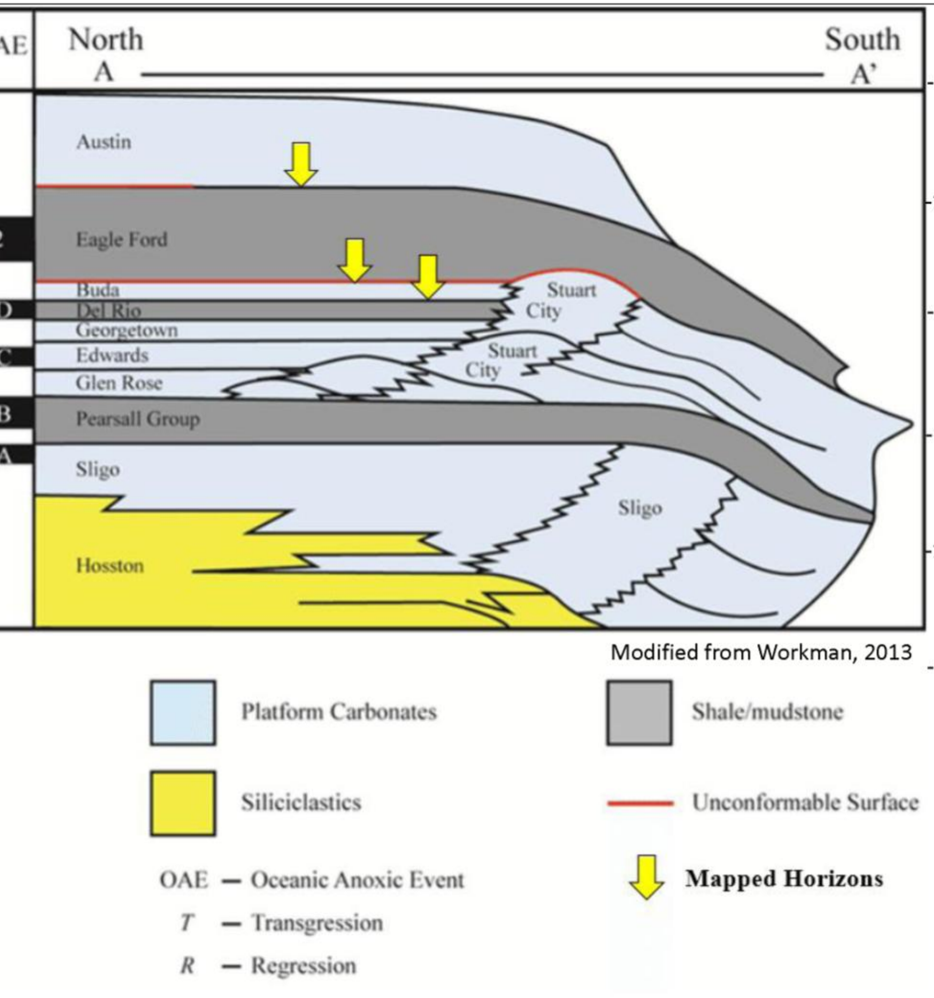

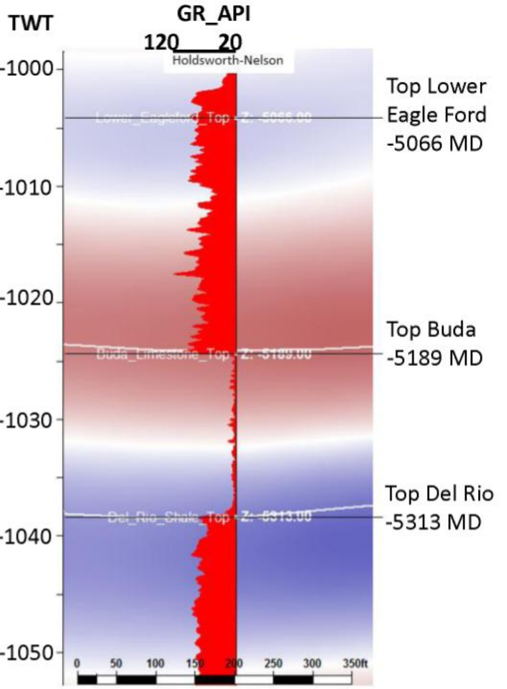

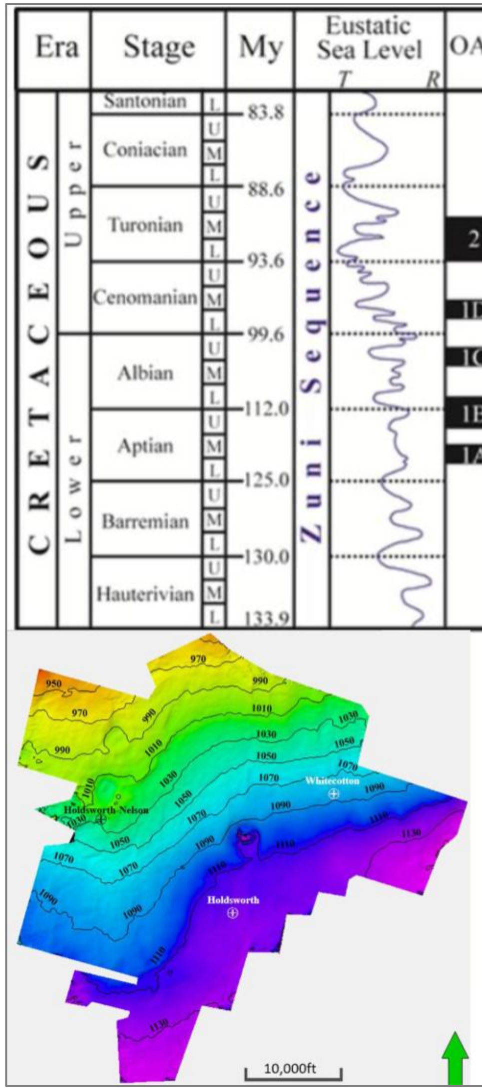

- Gamma Ray log displayed in Holdsworth-Nelson well
- Background fill is seismic amplitude

Presenter's notes: Comanche Shelf Depositional Architecture from the Hauterivian to Santonian Stages which primary developed large deposits of carbonates capped by thin successions of transgressive shales. (Workman, 2013).

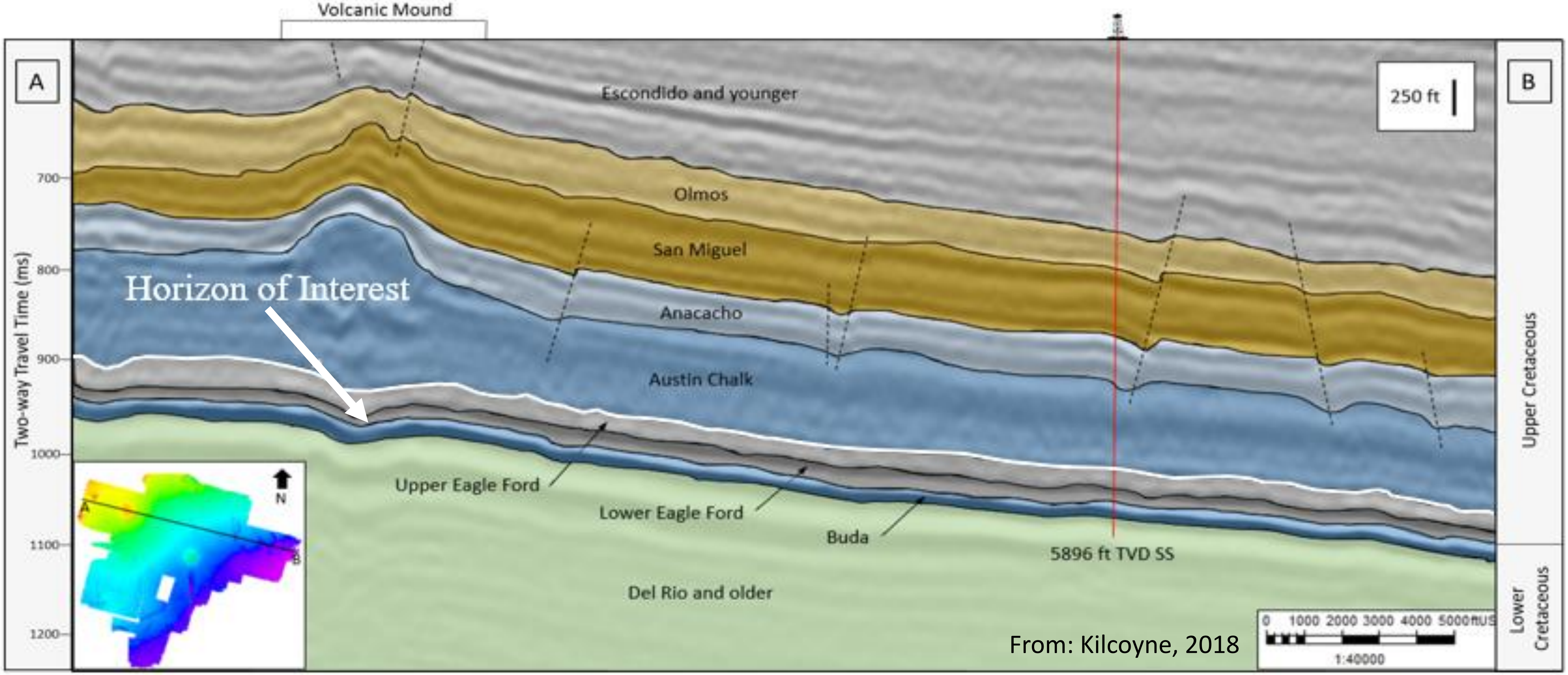

From: Kilcoyne, 2018

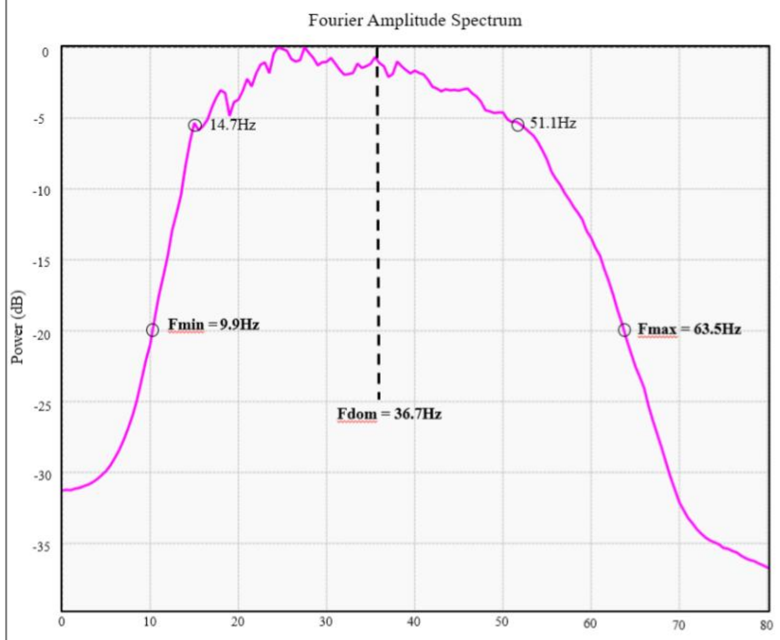

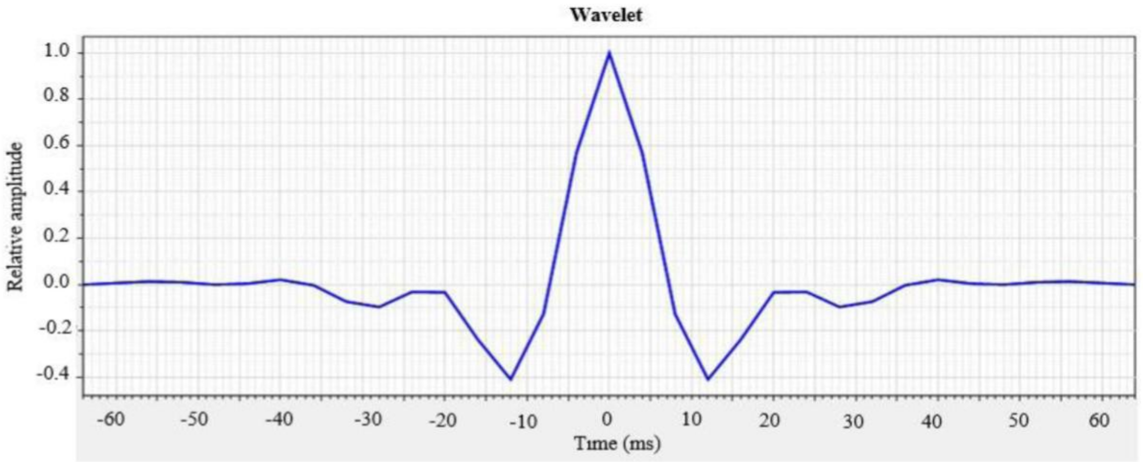

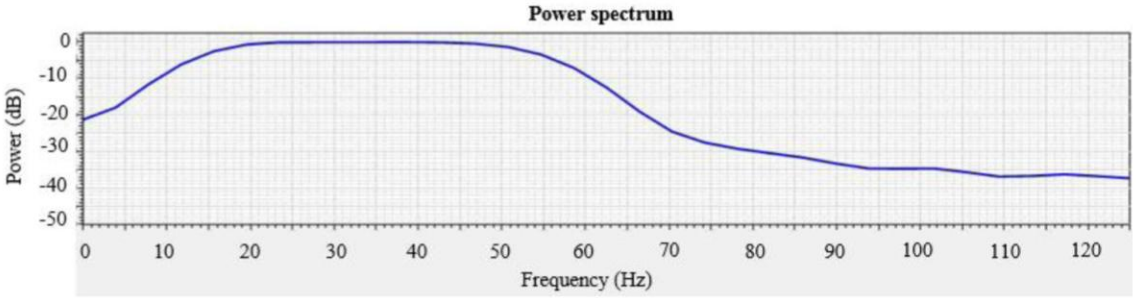

- Post stack time migration (4 ms sample rate)
- Average P-wave speed of Buda - 19000 ft/s
- Vertical resolution – 133 ft
- Horizontal resolution – 266 ft
- Ormsby wavelet scaled to corner frequencies

Presenter's notes: Fourier amplitude spectrum analysis showing min, max and dominant frequencies of Pedernales 3D survey over 2 second window centered on Buda limestone (-1050ms).

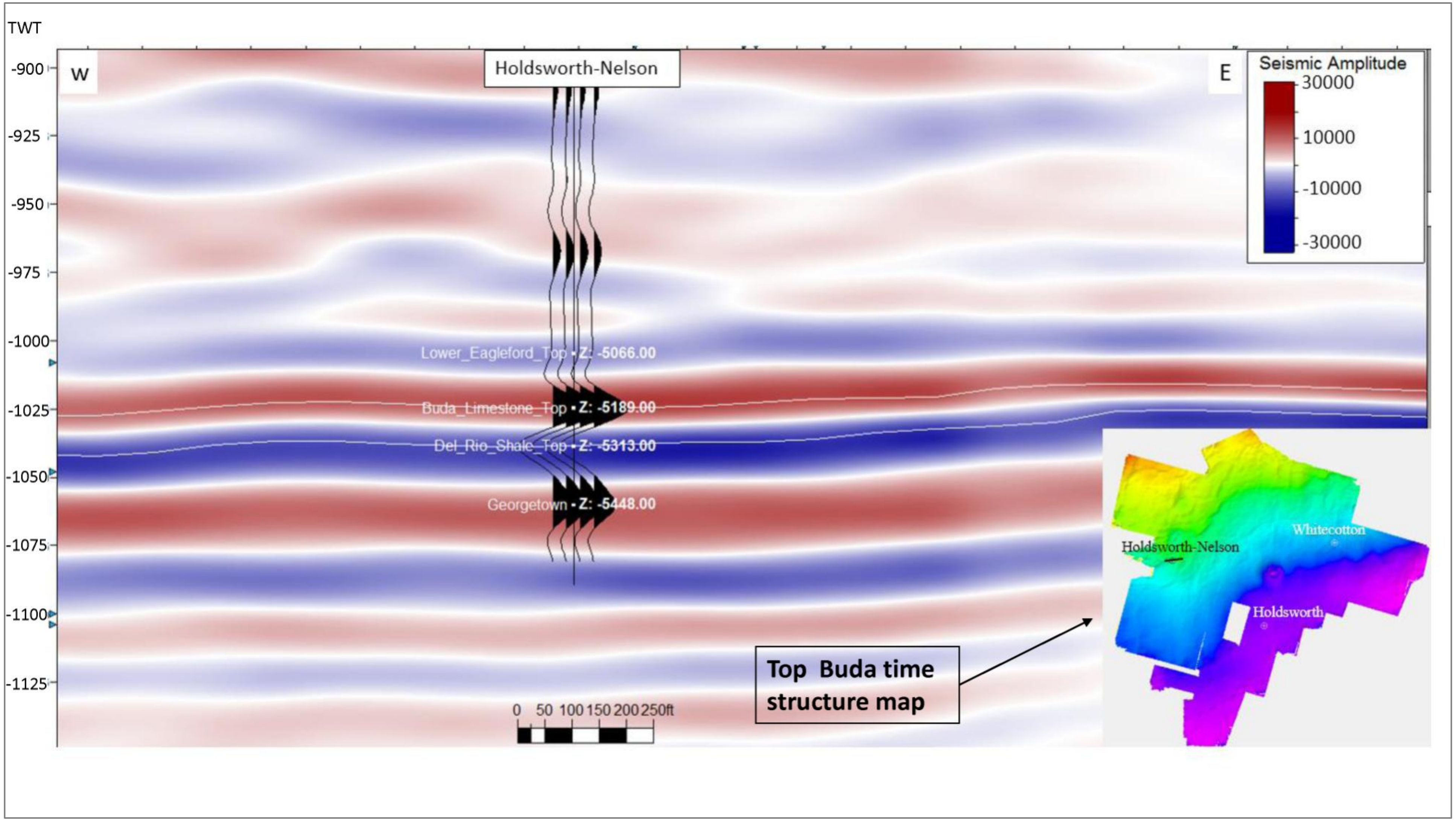

Presenter's notes: Synthetic seismogram displayed on seismic data showing a contact between Buda Limestone and Lower Eagle Ford represented by a strong peak and it's lower contact with Del Rio, represented by a trough. Horizons corresponding to top and bottom of Buda Limestone were tracked and displayed in white color.

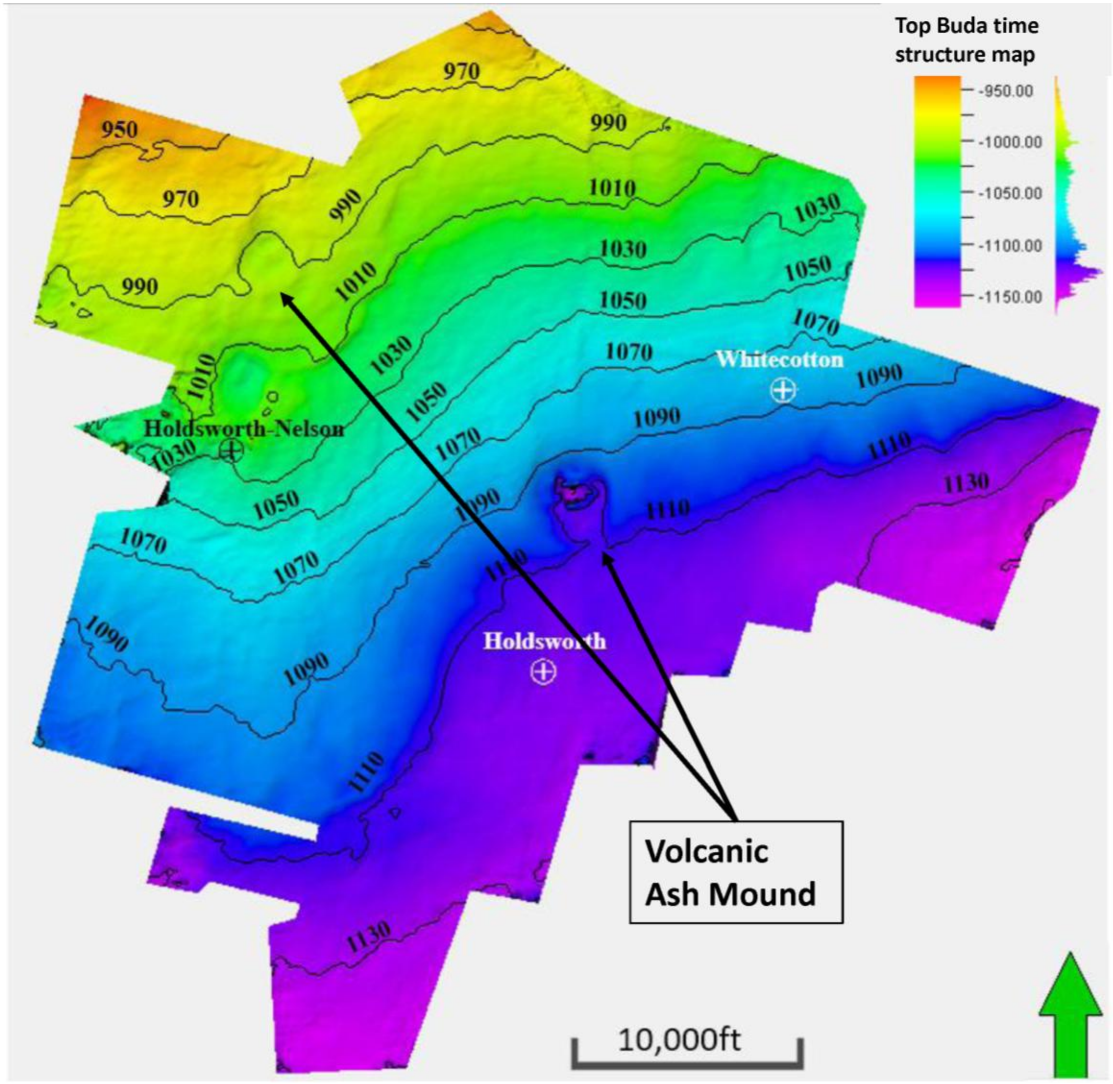

Presenter's notes: Buda limestone horizon time structure map with contours and well control.

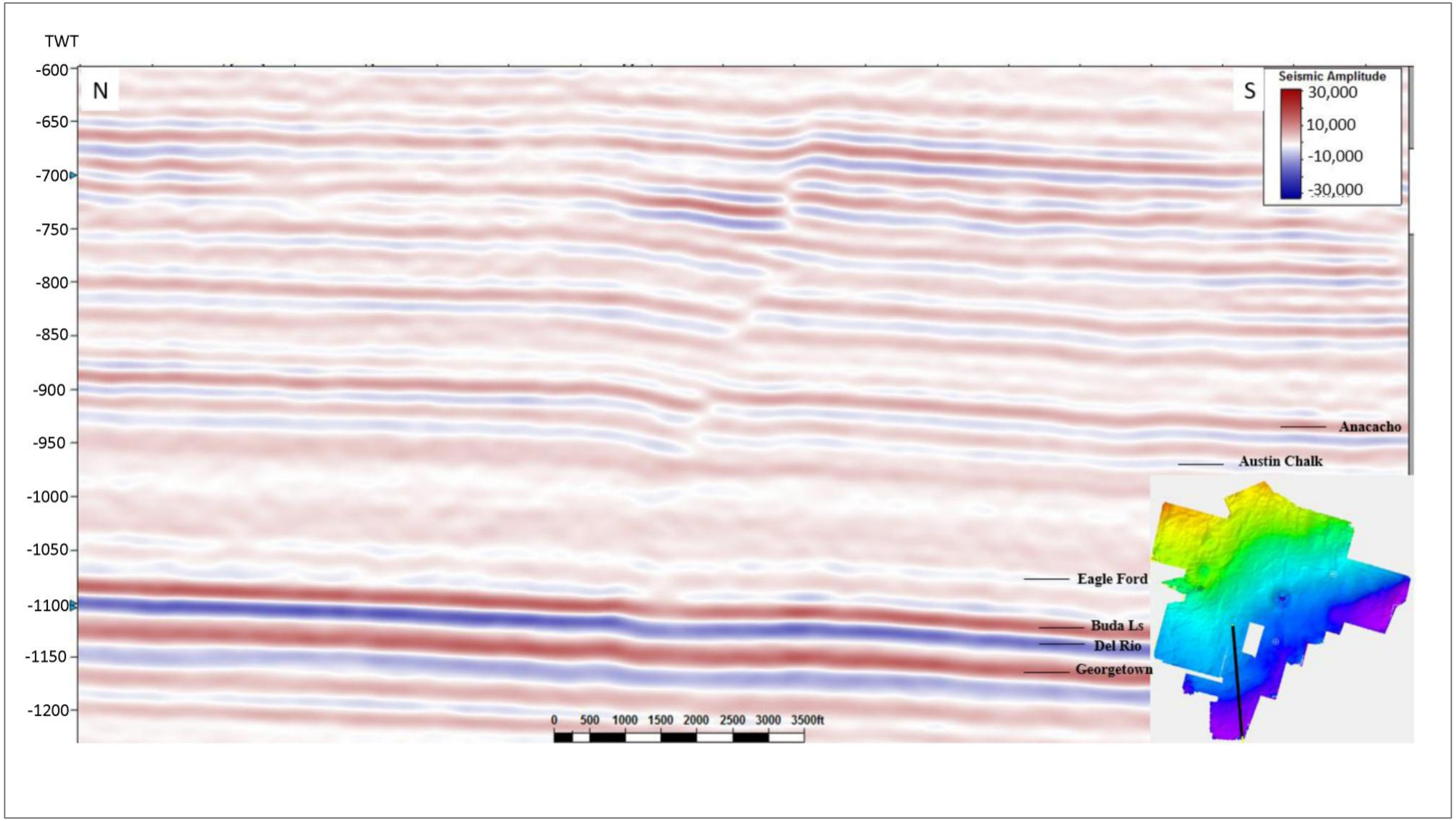

Presenter's notes: Typical structural behavior of Buda which forms a "step" feature right below a fault in formations above. The "step" feature is expected to follow a pattern and move down as a footwall above moves down, however Buda is being displaced upwards instead.

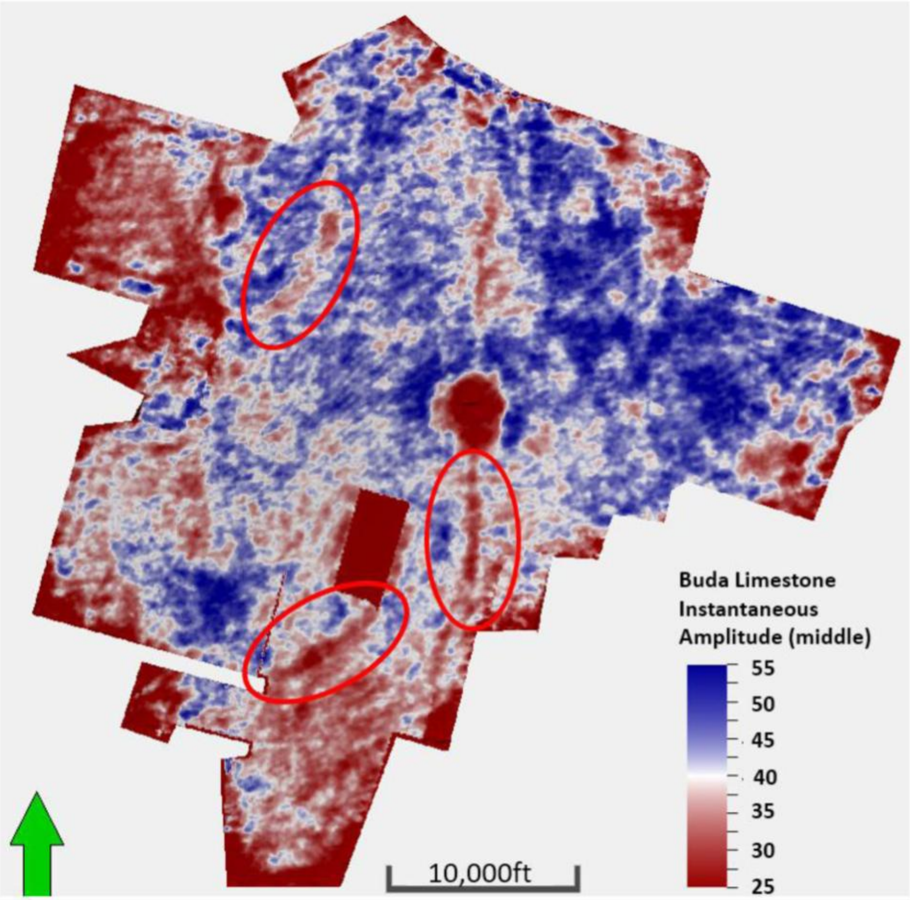

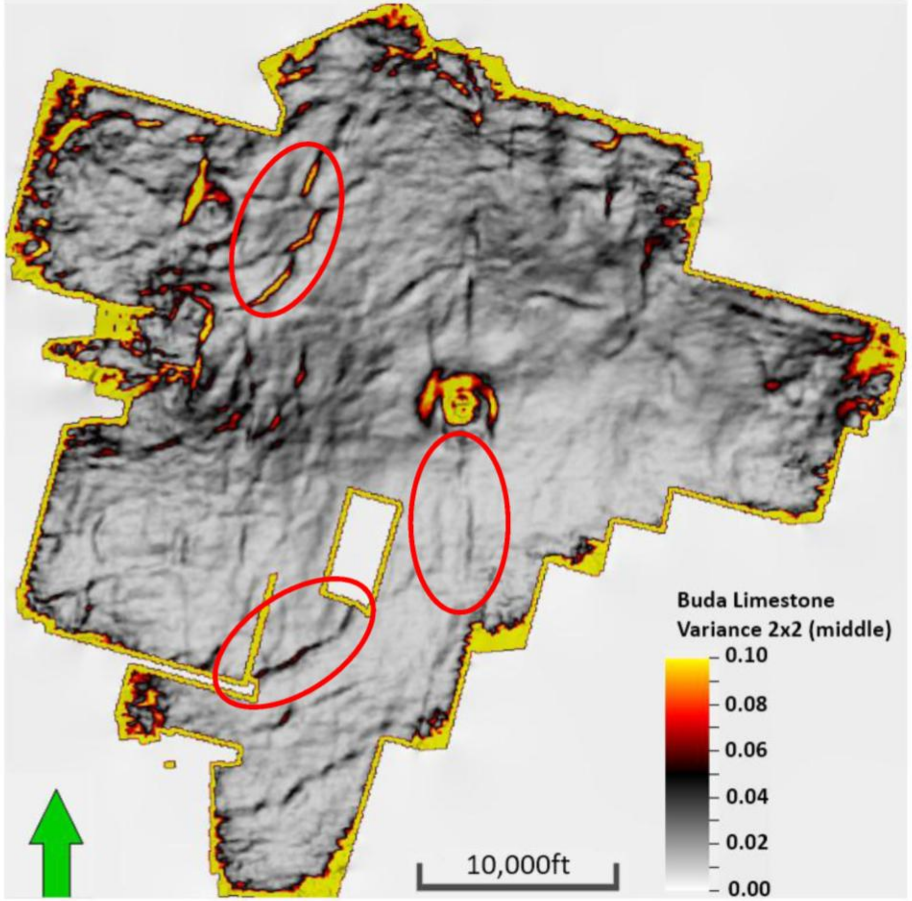

- Low values of Instantaneous Amplitude can be correlated to areas with “softer” lithology or enhanced porosity (Holman, 2014)
- Variance is an edge detection attribute capable of imaging discontinuities relating to faulting (Koson et al, 2014)

Presenter’s notes: Instantaneous amplitude calculated at the top of Buda limestone shows lower values (red colors) in areas of flexures and “step” features.

Most positive curvature

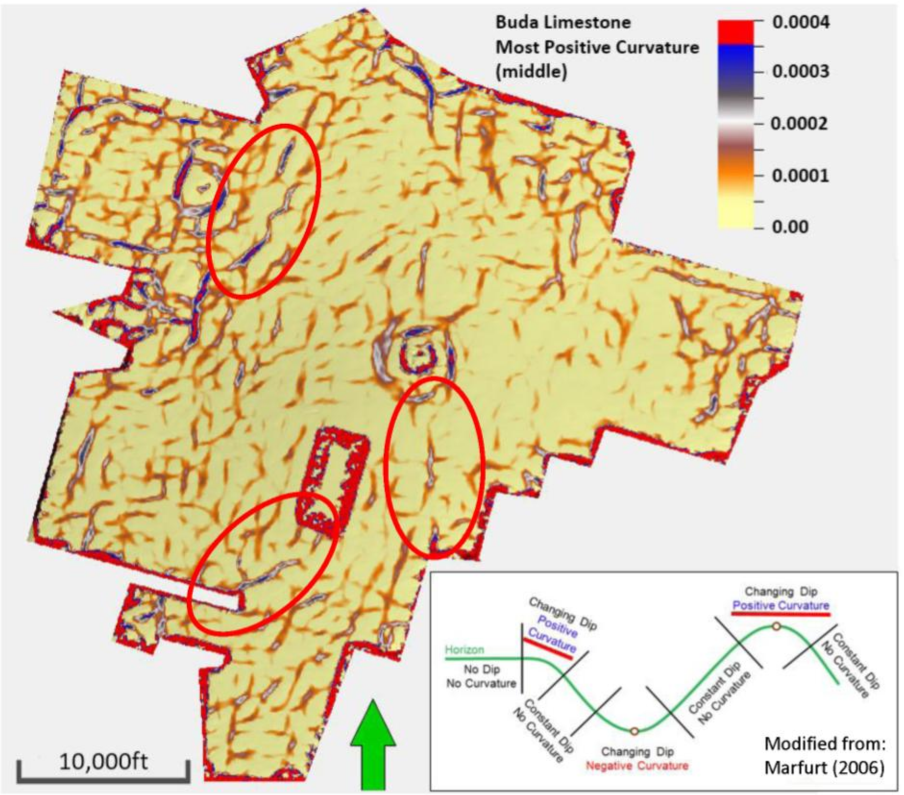

Most negative curvature

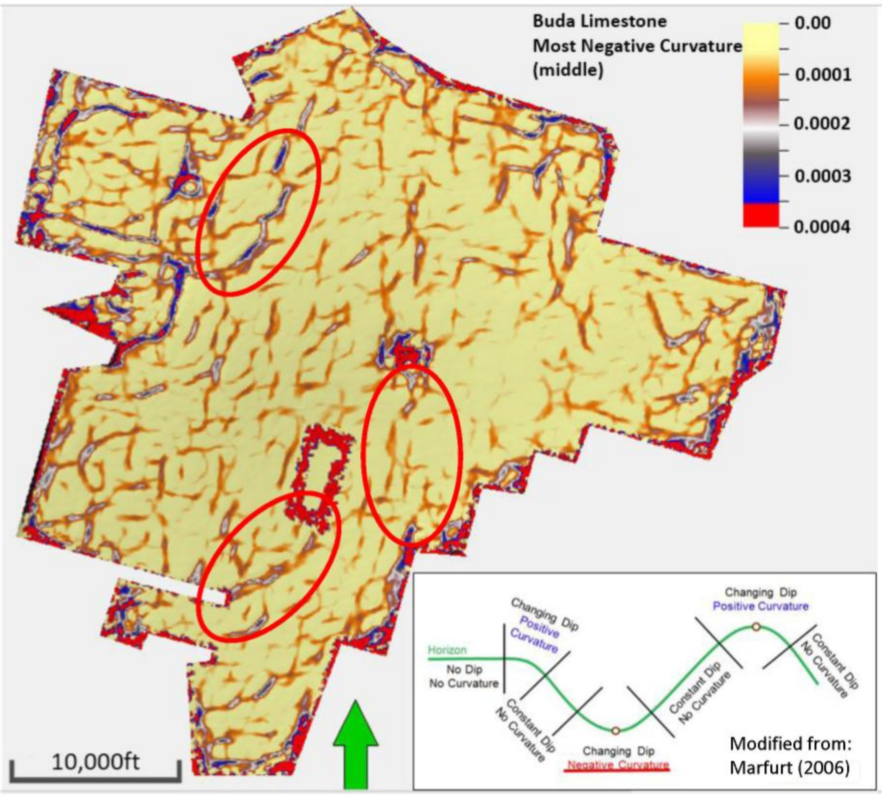

- Curvature measures the amount of surface deformation at a specific point, these observations can identify areas favorable to natural fracturing (Chopra and Marfurt, 2007).
- Original seismic has been preconditioned using following filters: median filter, frequency filter, Gaussian filter.

Presenter's notes: Most positive short wavelength curvature extracted through the middle of Buda Limestone. Areas with higher curvature values suggest that the surface of Buda is forming an anticline shape at that particular point.

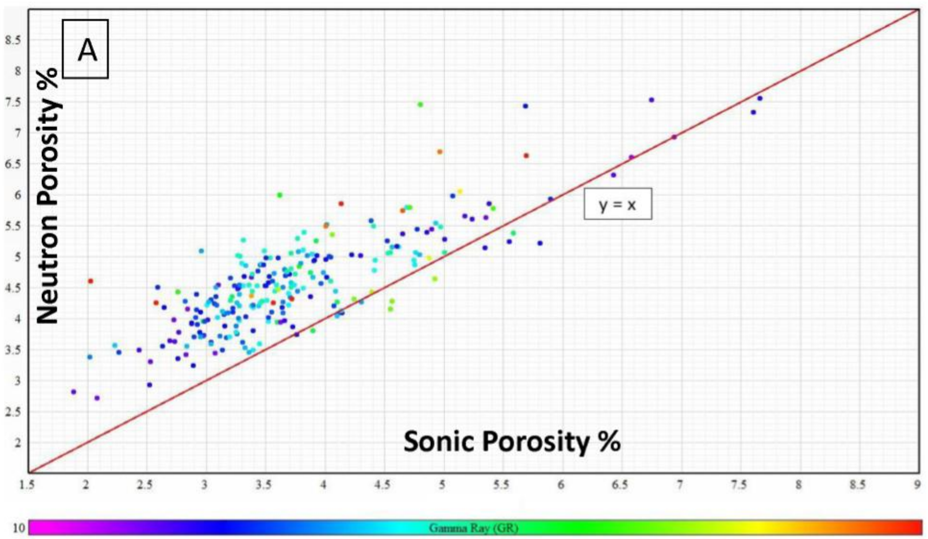

- In carbonates, Neutron porosity measures total porosity and Sonic measures matrix porosity.
- Values have been recorded in Holdsworth-Nelson well over the Buda Interval (5189 MD – 5313 MD).
- A – Neutron porosity plotted against Sonic Porosity
- B – Neutron porosity plotted against Acoustic Impedance (R^2 = 0.8089)
- C – Sonic porosity plotted against Acoustic Impedance (R^2 = 0.9320)

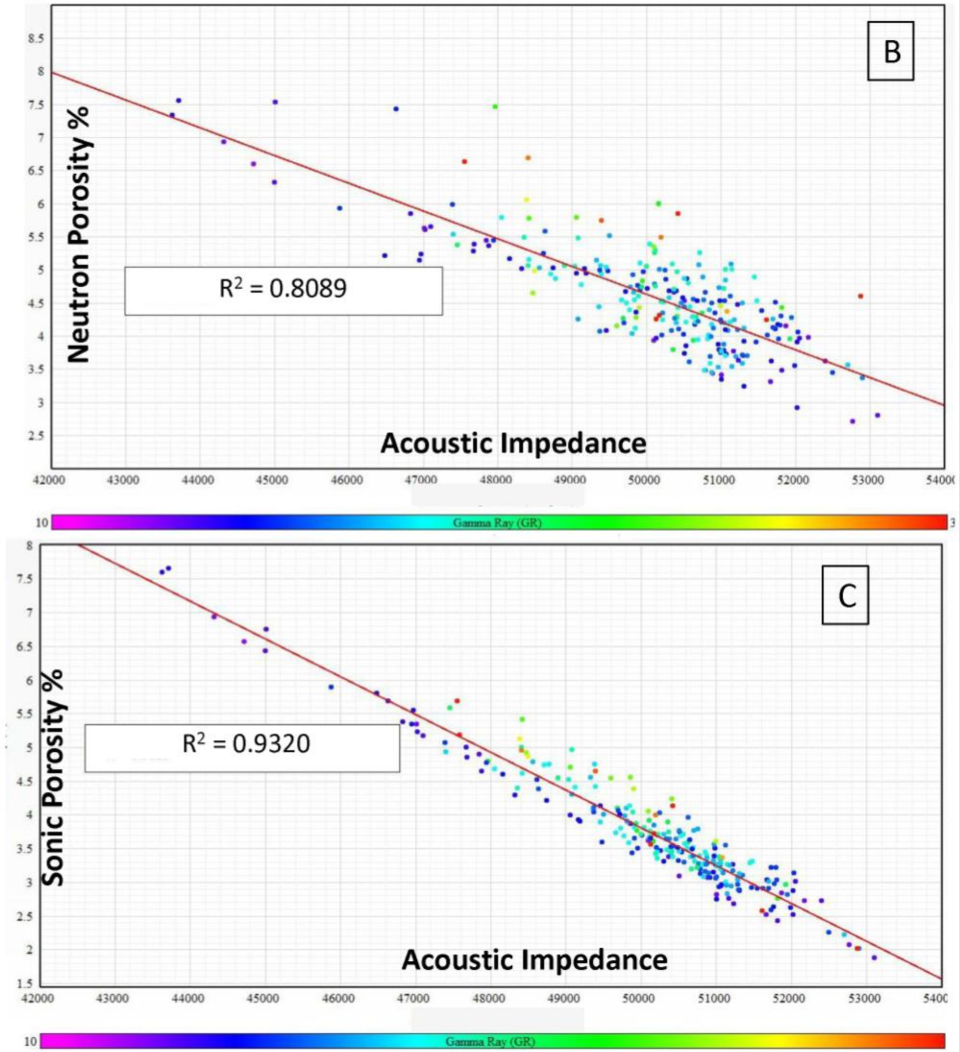

Presenter's notes: Cross plot establishing linear relationship between sonic porosity and acoustic impedance at the Holdswoth-Nelson well by linear regression equation with R value of 93%. Acoustic Impedance was calculated at the Holdsworth-Nelson well location using sonic and density logs. Both of these logs did not require correction at the Buda interval. In fractured carbonates, sonic porosity is an indicator of matrix porosity.

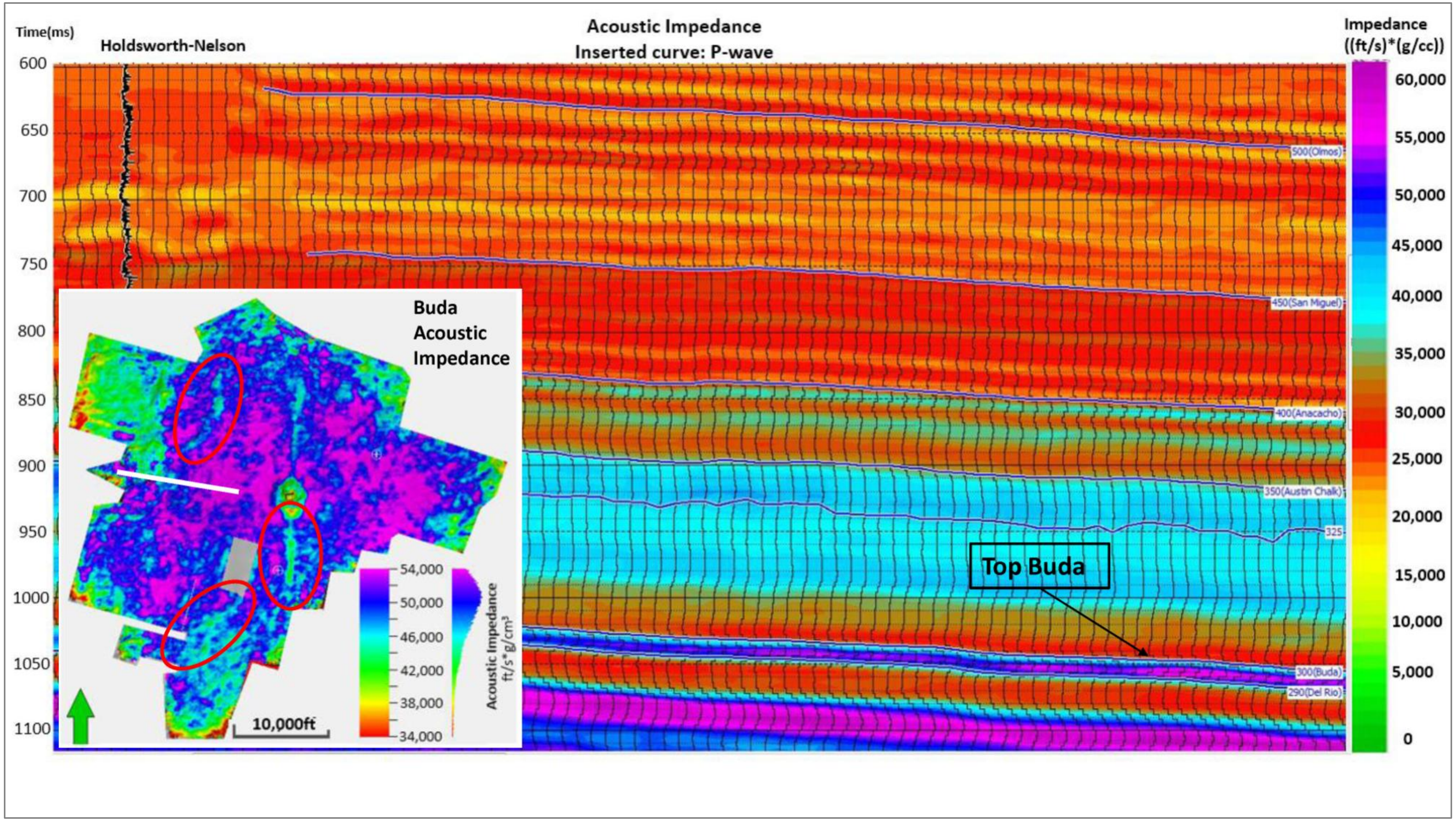

Presenter's notes: Initial Acoustic impedance model generated from low-frequency filtering of the Holdsworth-Nelson well.

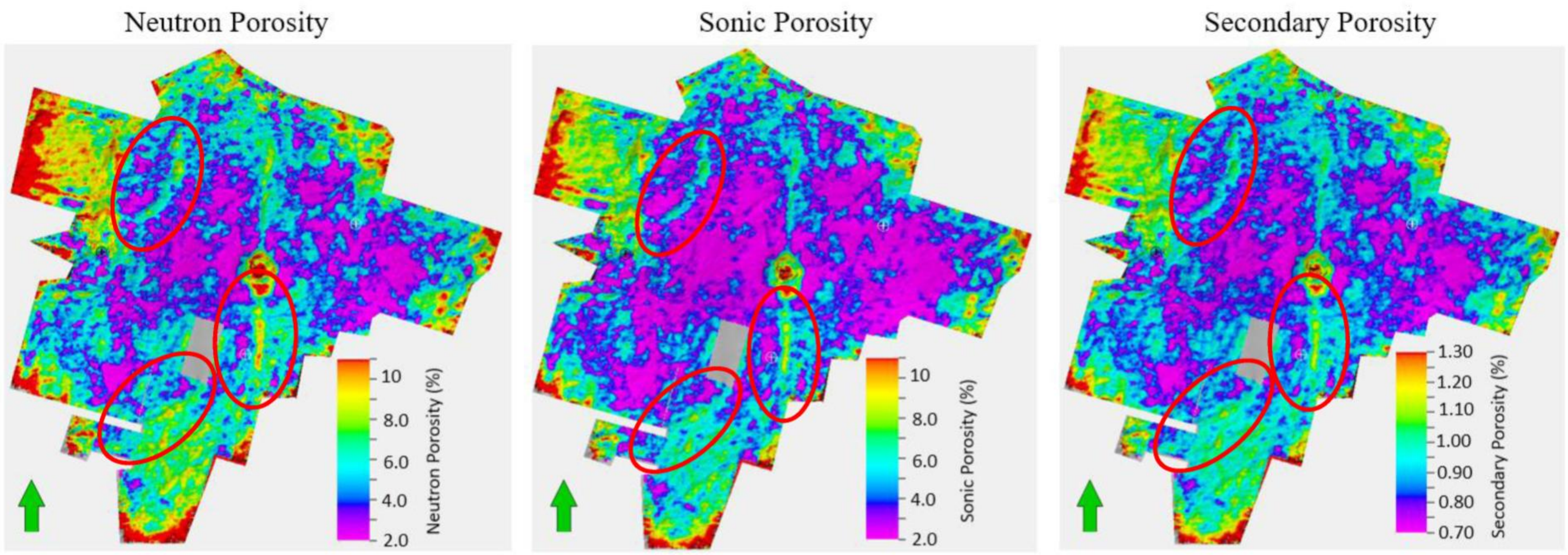

- Using the linear relationship between acoustic impedance and porosity, both sonic and neutron have been scaled to the whole Buda Interval
- By subtracting Sonic porosity from Neutron, it is possible to obtain secondary porosity values

Presenter's notes: Comparison between neutron, sonic and secondary porosity values in middle Buda Limestone (-7ms from the top).

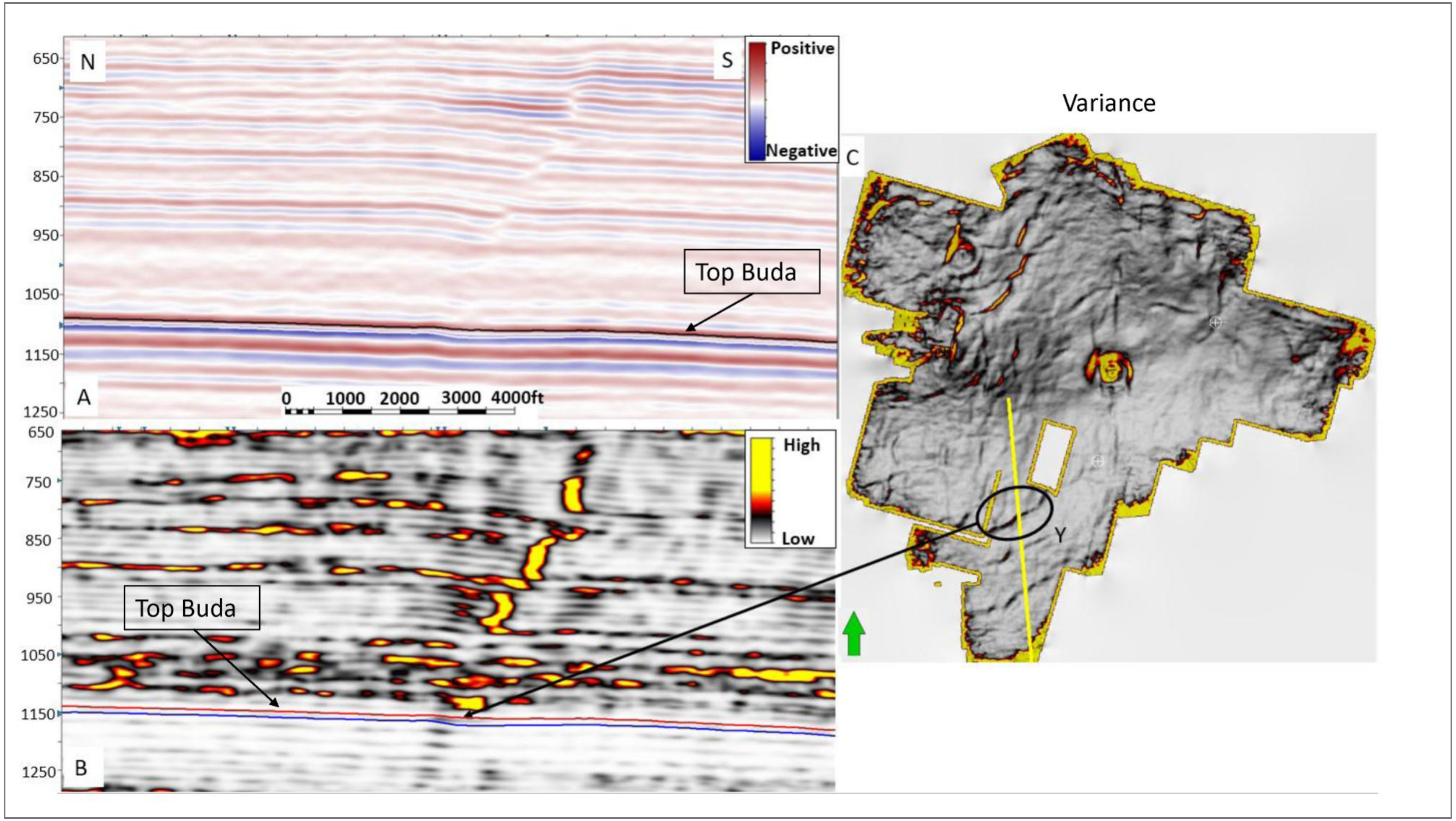

Presenter's notes: Comparison between amplitude and variance in cross section at the fault "Y" location. A – Amplitude seismic, B – Variance attribute, C – Variance attribute time slice through middle Buda.

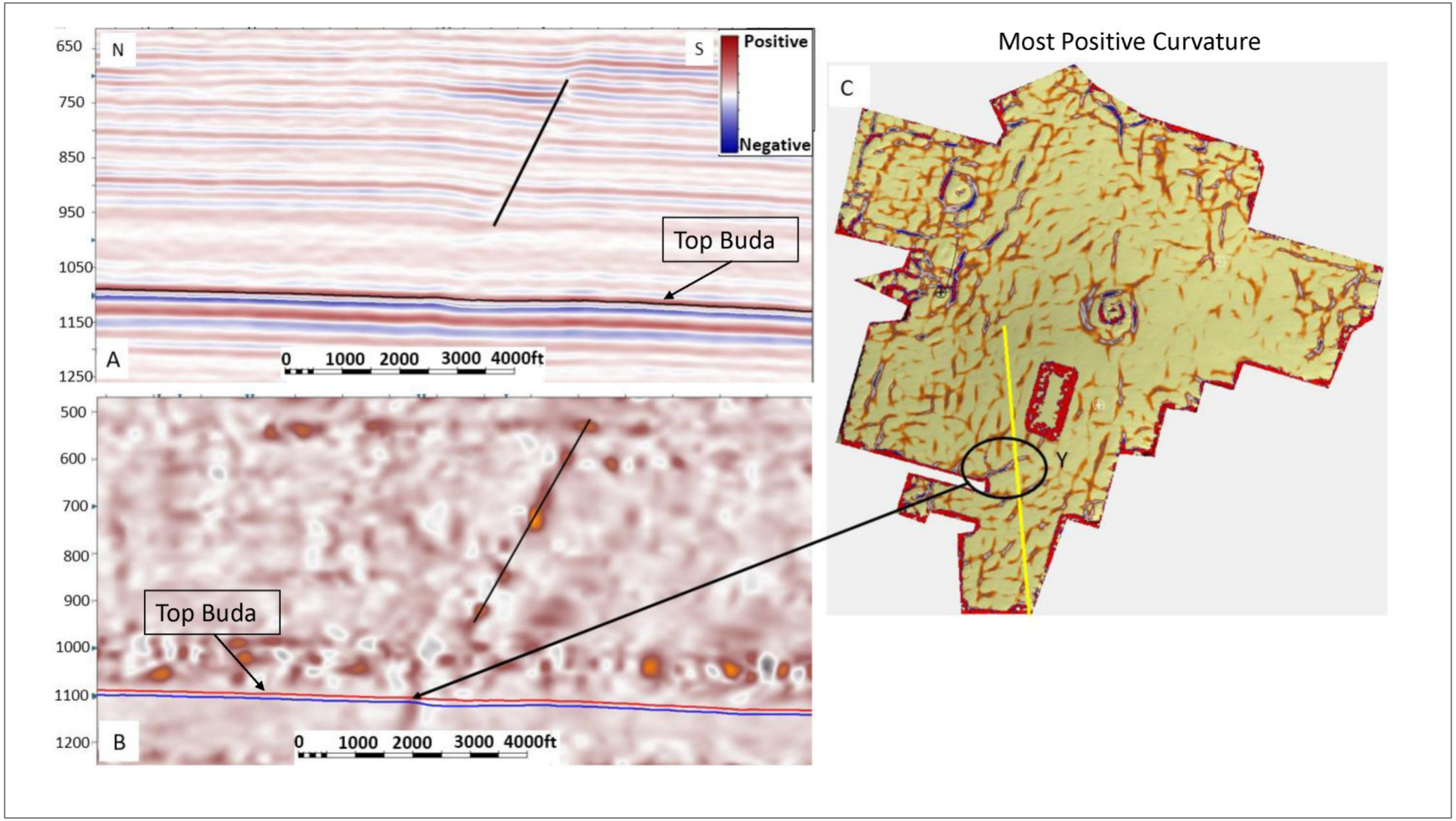

Presenter's notes: Comparison between amplitude and most positive curvature in cross section at the fault "Y" location. A – Amplitude seismic, B – most positive curvature attribute, C – most positive curvature attribute time slice through middle Buda.

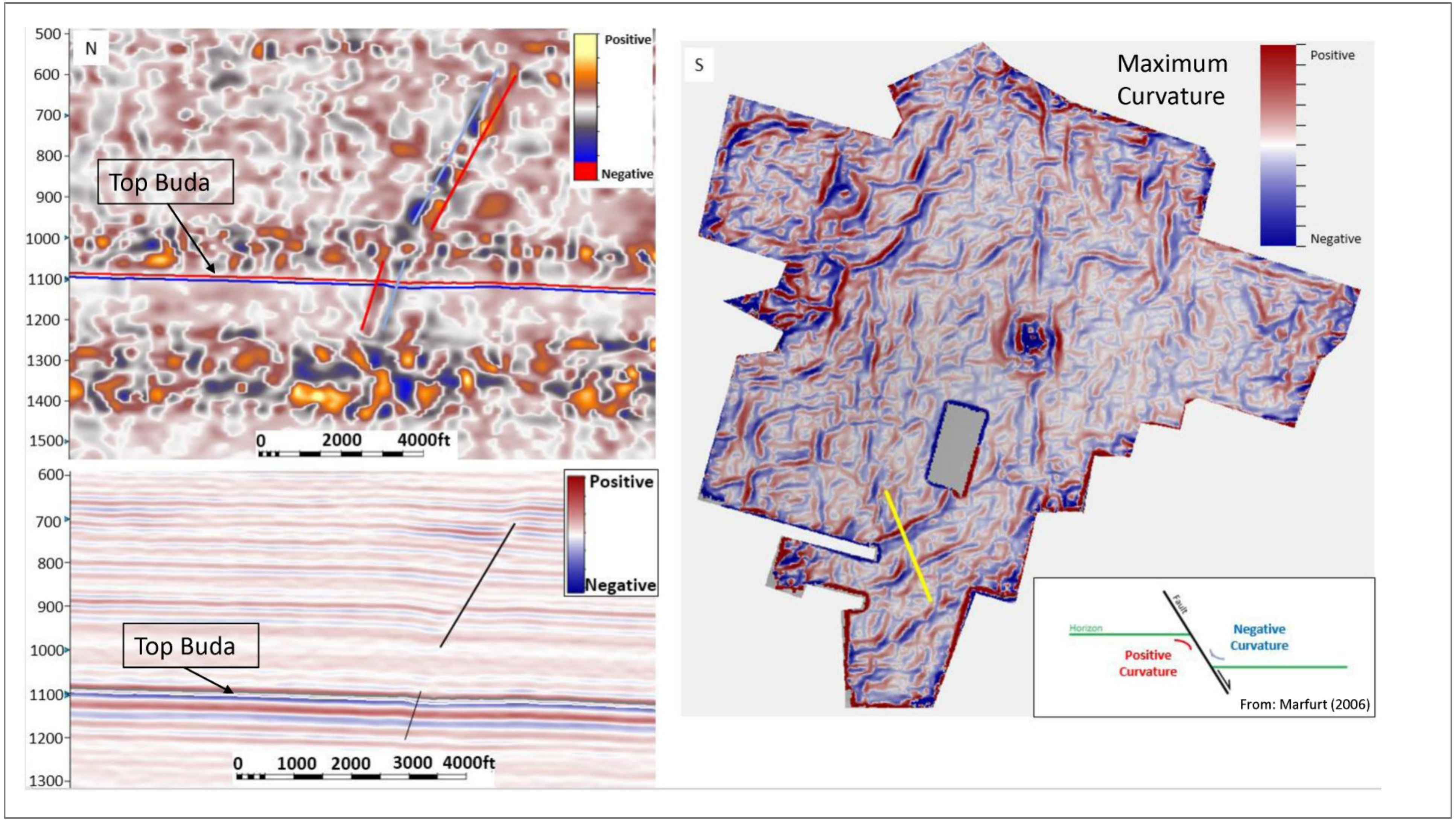

Presenter's notes: Maximum volumetric curvature at the fault location. The fault in upper formations changes curvature values from negative to positive suggesting that downthrown side is to the North, while lower fault penetrating Buda limestone has curvature values that change from positive to negative suggesting downthrown side to the south.

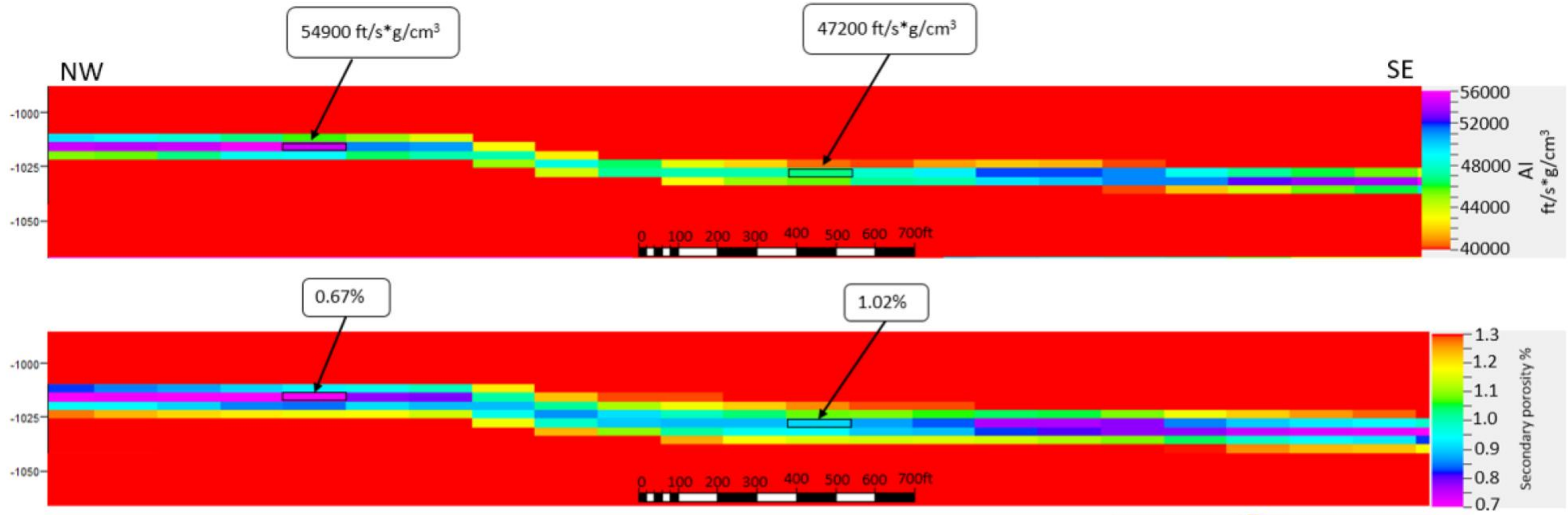

- Acoustic Impedance volume displayed, has been tuned specifically to Buda Limestone interval

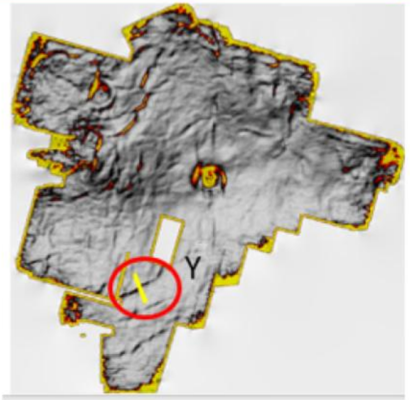

Presenter's notes: Cross sectional view of acoustic impedance (top) and secondary porosity (bottom) with turned off interpolation at the fault "X" location. Decrease in acoustic impedance on the downthrown side of the block is correlated with increased secondary porosity at the same spot.

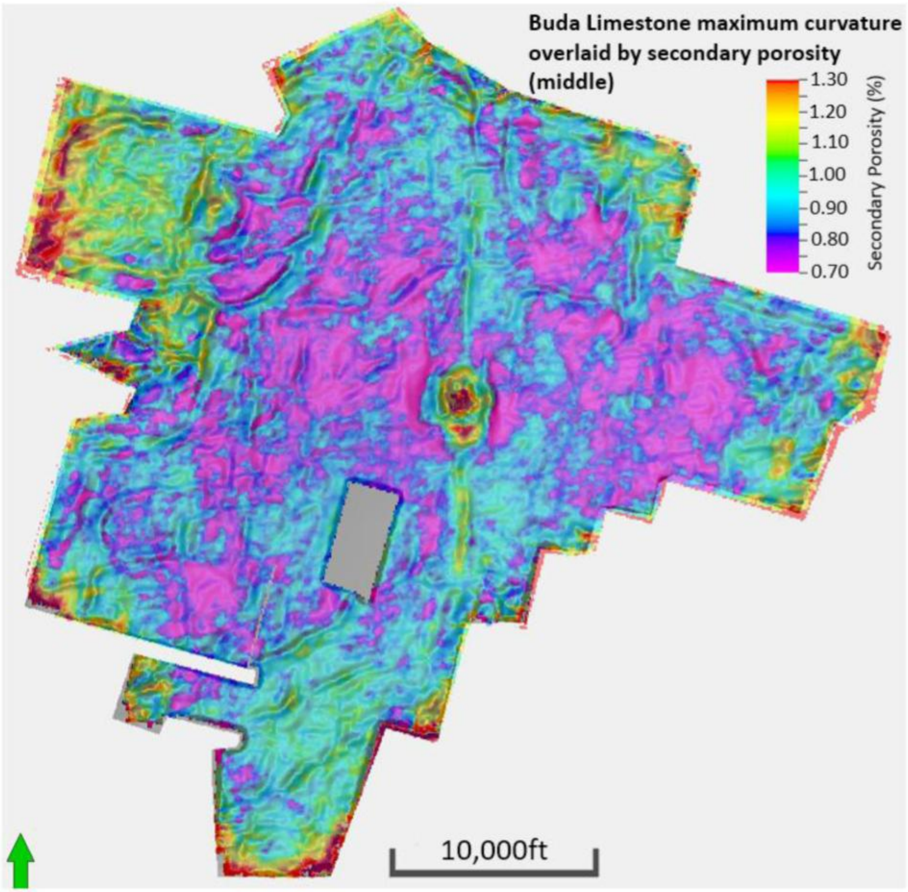

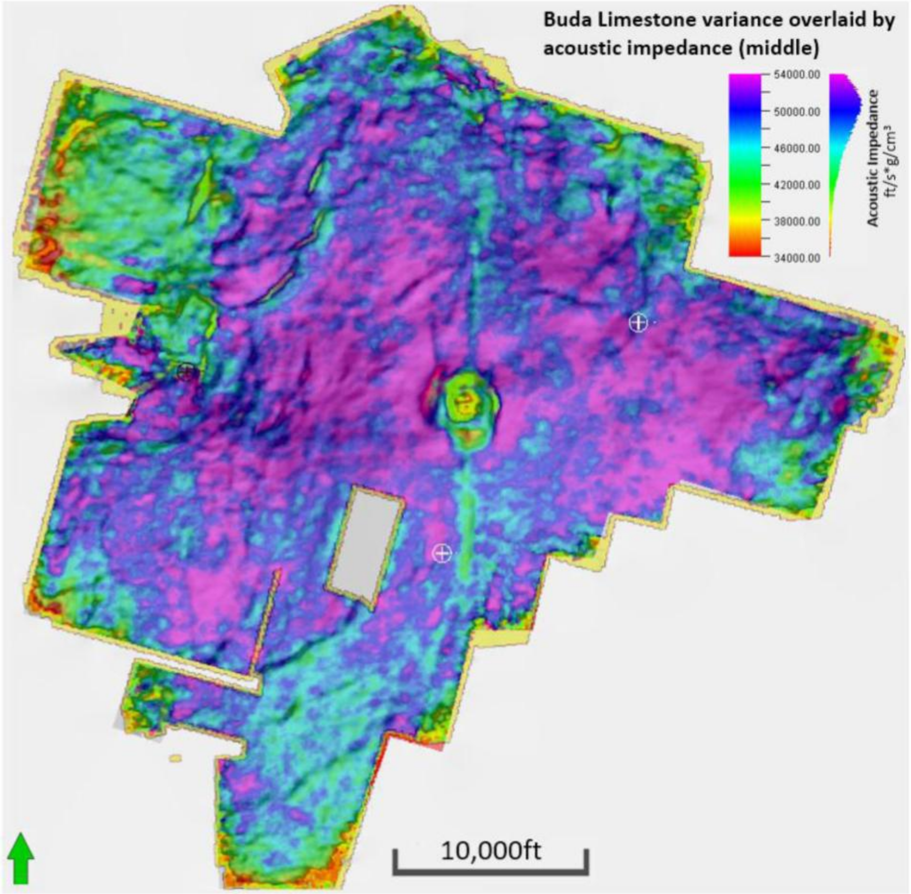

Presenter’s notes: Secondary porosity overlaid with maximum curvature demonstrating relationship between faulting and increased secondary porosity values on downthrown side of the block.

Thank you!

- Schlumberger for providing Petrel and Techlog software
- CGG for providing Hampson-Russel
- Stephens Production company for providing the seismic data and well logs
- Dr. Christopher Liner for countless hours of his effort and help